

Inhibition of lncRNA *MIR31HG* Promotes Osteogenic Differentiation of Human Adipose-Derived Stem Cells

CHANYUAN JIN,^{a,e} LINGFEI JIA,^{b,c} YIPING HUANG,^d YUNFEI ZHENG,^d NING DU,^c
YUNSONG LIU,^a YONGSHENG ZHOU^{a,e}

Key Words. lncRNA *MIR31HG* • NF- κ B • Human adipose-derived stem cells • Osteogenic differentiation

^aDepartment of Prosthodontics, ^bDepartment of Oral and Maxillofacial Surgery, ^cCentral Laboratory, ^dDepartment of Orthodontics, ^eNational Engineering Lab for Digital and Material Technology of Stomatology, Peking University School and Hospital of Stomatology, Beijing Key Laboratory of Digital Stomatology, Beijing, China

Correspondence: Yongsheng Zhou, D.D.S., Ph.D., Department of Prosthodontics, Peking University School and Hospital of Stomatology, 22 Zhongguancun South Avenue, Haidian District, Beijing 100081, China. Telephone: +86-10-82195370; Fax: +86-10-62173402; e-mail: kqzhouysh@hsc.pku.edu.cn

Received January 26, 2016; accepted for publication May 30, 2016; first published online in *STEM CELLS EXPRESS* June 22, 2016.

© AlphaMed Press
1066-5099/2016/\$30.00/0

[http://dx.doi.org/
10.1002/stem.2439](http://dx.doi.org/10.1002/stem.2439)

ABSTRACT

Osteogenic differentiation and bone formation is suppressed under condition of inflammation induced by proinflammation cytokines. A number of studies indicate miRNAs play a significant role in tumor necrosis factor- α -induced inhibition of bone formation, but whether long non-coding RNAs are also involved in this process remains unknown. In this study, we evaluated the role of *MIR31HG* in osteogenesis of human adipose-derived stem cells (hASCs) in vitro and in vivo. The results suggested that knockdown of *MIR31HG* not only significantly promoted osteogenic differentiation, but also dramatically overcame the inflammation-induced inhibition of osteogenesis in hASCs. Mechanistically, we found *MIR31HG* regulated bone formation and inflammation via interacting with NF- κ B. The p65 subunit bound to the *MIR31HG* promoter and promoted *MIR31HG* expression. In turn, *MIR31HG* directly interacted with I κ B α and participated in NF- κ B activation, which builds a regulatory circuitry with NF- κ B. Targeting this *MIR31HG*-NF- κ B regulatory loop may be helpful to improve the osteogenic capacity of hASCs under inflammatory microenvironment in bone tissue engineering. *STEM CELLS* 2016; 00:000–000

SIGNIFICANCE STATEMENT

In the condition of bone loss, the defective or injured tissues are often associated with inflammation. We identify that knockdown of *MIR31HG* not only promoted osteogenic differentiation but also reversed the inflammation-induced inhibition of bone formation. And we find the novel regulatory circuitry between *MIR31HG* and the NF- κ B. *MIR31HG* is induced by nuclear translocation of NF- κ B, and *MIR31HG*, in turn, directly binds to I κ B α and contributes to I κ B α phosphorylation and NF- κ B activation. Thus, knockdown of *MIR31HG* expression can be an approach to improve bone regeneration and may have a broad future in clinical applications.

INTRODUCTION

Human adipose-derived stem cells (hASCs) are a type of adult mesenchymal stem cell (MSC) capable of bone regeneration and repair. As they can be obtained from adipose tissues by a more abundant and less invasive procedure, hASCs have become an attractive source of stem cells in bone tissue engineering [1, 2]. A number of studies have shown the ability of ASCs to repair bone defects in animal models [3, 4], but most of these experiments were performed under minimal inflammation. However, in therapeutic bone regeneration, the defective or injured tissues are frequently in an inflamed condition [5]. Moreover, growing evidence suggests that MSC differentiation is precisely regulated by the molecular signals from the extracellular environment [6, 7], and that the

proinflammatory cytokines in the cell microenvironment inhibit osteogenic differentiation and bone formation [8]. Thus, it is necessary to overcome the inflammation-induced inhibition of osteogenesis in bone tissue regeneration.

Bone remodeling is a continuous process that depends on the balance of osteoclast-mediated bone resorption and osteoblast-mediated bone formation. The inflammatory cytokines disrupt normal bone homeostasis, impair bone formation, and induce bone loss in inflammatory diseases. Several molecular pathways related to osteoblast differentiation are dysregulated under inflammatory environment, such as the mitogen-activated protein kinase [9], nuclear factor- κ B (NF- κ B) [10], bone morphogenetic protein (BMP) [11], and Wnt signaling pathway [12]. Among these, NF- κ B is a key

regulator of inflammation, and is activated by tumor necrosis factor- α (TNF- α), interleukin-17 (IL-17), and lipopolysaccharides. Growing evidence has showed that NF- κ B signaling inhibits osteoblast (OB) differentiation and bone formation [13, 14], while specific inhibition of NF- κ B in differentiated osteoblasts significantly enhanced bone matrix formation and mineral density [15]. Recently, non-protein-coding RNAs (ncRNAs) have emerged as important regulatory transcripts in biological control and pathology [16]. Small ncRNAs, including miR-17 [17], miR-21 [18], miR-23a [19], and miR-155 [20], have been implicated in the TNF- α -induced inhibition of bone formation. By contrast, the function of long non-coding RNAs (lncRNAs), tentatively defined as ncRNAs >200 nt in length [21, 22], are largely unknown in MSC osteogenic differentiation under inflammatory conditions. Recent studies have shown that the lncRNAs *Lethe* [23] and *NKILA* [24] directly interact with the NF- κ B complex in inflammatory diseases, implying that lncRNAs are important for the NF- κ B signaling pathway.

In this study, we aimed to investigate the role of lncRNA (*MIR31HG*) in inflammation-mediated bone metabolism. *MIR31HG* (previously known as *LOC554202*), located on chromosome 9 (9p21.3), is demonstrated to affect cell proliferation, differentiation, and motility in tumor development [25, 26]. However, the role of *MIR31HG* in inflammation or bone formation has not been reported. Since a previous study has shown that the *MIR31HG* promoter contains putative NF- κ B binding sites [27], we hypothesized that *MIR31HG* may be involved in the NF- κ B-mediated inhibition of osteogenesis. In this study, we identified that the lncRNA *MIR31HG*, induced by NF- κ B, is also involved in an NF- κ B regulatory feedback loop. Importantly, knockdown of *MIR31HG* not only significantly promotes osteogenic differentiation of hASCs, but also reverses the inflammation-induced inhibition of osteogenesis and bone formation.

MATERIALS AND METHODS

Cell Culture

Primary hASCs were obtained from ScienCell (San Diego, CA) and cultured in proliferation media (PM) consisting of DMEM with 10% fetal bovine serum and 1% antibiotics. Stem cells from three donors were used for the in vitro and in vivo experiments. All cell-based in vitro experiments were repeated in triplicate. For the osteogenic differentiation experiment, cells were induced in osteogenic media (OM) containing standard PM supplemented with 100 nM dexamethasone, 0.2 mM ascorbic acid, and 10 mM β -glycerophosphate. The 293T cells were obtained from American Type Culture Collection (Manassas, VA) and cultured in DMEM supplemented with 10% fetal bovine serum and 1% antibiotics.

Lentivirus Infection

Recombinant lentiviruses containing full-length *MIR31HG* and the scramble control (NC) were obtained from Integrated Biotech Solutions Co. (Ibsbio Co., Shanghai, China). Recombinant lentiviruses targeting *MIR31HG* (sh*MIR31HG*-1 and sh*MIR31HG*-2) and the scramble control (shNC) were obtained from GenePharma Co. (Shanghai, China). Transfection of the hASCs was performed by exposing them to dilutions of the viral supernatant in the presence of polybrene (5 μ g/ml) for 72 h.

Alkaline Phosphatase Staining and Activity

Cells cultured for 7 days under PM or OM were assayed for alkaline phosphatase (ALP) staining and activity, as described previously [28, 29]. ALP staining was performed according to the protocol of the NBT/BCIP staining kit (CoWin Biotech, Beijing, China). ALP activity was analyzed using an ALP activity colorimetric assay kit (Biovision, Milpitas, CA). Total protein was determined in the same sample with the BCA method using the Pierce protein assay kit (Thermo Fisher Scientific, Rockford, IL). ALP activity relative to the control treatment was calculated after normalization to the total protein content.

Alizarin Red S Staining and Quantification

Cells cultured for 14 days under PM or OM were assayed as described previously [28, 29]. The cultured cells were fixed with 4% paraformaldehyde and then stained with 0.1% Alizarin red S pH 4.2 (Sigma-Aldrich, Saint Louis, MO) for 20 min. For quantitative assessment of the degree of mineralization, the stain was eluted by 100 mM cetylpyridinium chloride (Sigma-Aldrich) for 1 hour and quantified by spectrophotometric absorbance at 570 nm. Alizarin red S intensity relative to the control treatment was calculated after normalization to the total protein content.

Von Kossa Staining

Cells cultured for 14 days under PM or OM were assessed using the von Kossa staining method as described previously [30]. Briefly, cells were fixed with 4% paraformaldehyde and then incubated with 5% silver nitrate solution for 30 minutes in the dark, followed by exposure to UV light. Unincorporated silver nitrate was removed using 5% sodium thiosulfate, followed by several washes with water.

RNA Oligoribonucleotide, Chemicals, and Transient Transfection

Small-interfering RNAs (siRNA) targeting the *MIR31HG*, p65, p50, I κ B α , and the scramble control (si-NC) were purchased from Integrated Biotech Solutions Co. The sequences are listed in Supporting Information Table 1. For transient transfection, cells were cultured and grown to 70–80% confluence, then transfected with plasmids or siRNA using Lipofectamine 2000 (Invitrogen, Carlsbad, CA) according to the manufacturer's procedure.

The recombinant human TNF- α and IL-17 were purchased from PeproTech Inc. (Rocky Hill, NJ). The specific NF- κ B inhibitor, BAY117082, was obtained from Sigma-Aldrich to inhibit I κ B α phosphorylation. Lithium chloride (LiCl), a GSK-3 β inhibitor, was obtained from Sigma-Aldrich to block β -catenin degradation. In the treatment group, TNF- α or IL-17 (10 ng/ml) was added to the culture media every 24 hours with or without BAY117082 (5 μ mol/l) or LiCl (5 mmol/l). For RNA and protein analyses, the cells were harvested within 24 hours. For osteogenic differentiation, the cells were harvested after 7 or 14 days.

Vectors

A 2,198 bp fragment of human *MIR31HG* promoter (–1,994 bp to +204 bp relative to the transcription start site) was amplified from the genomic DNA of HeLa cells and cloned into the PGL3-Enhancer vector (Promega, Madison, WI). The primers used to clone the *MIR31HG* promoter were as follows: sense, 5'-GCT AGC ACA AAG TCT TGC CTA GTG GGA TT-3' and antisense,

5'-CTC GAG GTC CGA GTA GGA GGA CAG AAG C-3'. A series of deletion of the *MIR31HG* promoter were constructed by Integrated Biotech Solutions Co. based on the full-length promoter reporter construct. The plasmid containing 5× NF-κB consensus-binding sites with luciferase reporter gene was a gift from Professor Zhong Chen (National Institutes of Health, Bethesda, MD) [31]. All constructs were confirmed by DNA sequencing.

Dual Luciferase Reporter Assay

Luciferase assays were performed as described previously [32]. For each transfection with subsequent reporter assay, the total quantity of transfected plasmid was kept constant by the addition of pRL-TK, a plasmid expressing renilla luciferase (Promega, Madison, WI). The renilla and firefly luciferase activities were measured 24 hours after transfection using the Dual Luciferase Reporter Assay System (Promega). All luciferase values were normalized by renilla luciferase and expressed relative to the basal activity as fold induction.

RNA Isolation and Quantitative Reverse Transcription-Polymerase Chain Reaction (qRT-PCR)

Total RNA was extracted using TRIzol reagent (Invitrogen) according to the manufacturer's procedure, and then reverse-transcribed into cDNA using a cDNA Reverse Transcription Kit (Applied Biosystems, Foster City, CA). Quantitative polymerase chain reaction was conducted with SYBR Green Master Mix (Life Technologies) as described on the ABI Prism 7500 real-time PCR System (Applied Biosystems) using GAPDH for normalization [33]. The primers used are listed in Supporting Information Table 1.

Immunofluorescence Staining

Immunofluorescence staining was performed as described previously [34]. Cells grown on sterile glass coverslips were fixed with 4% paraformaldehyde for 30 minutes, permeabilized with 0.1% Triton X-100 for 15 minutes, and then blocked with 5% normal goat serum for 30 minutes. Thereafter, cells were incubated with primary antibodies against osteocalcin (OCN, Abcam, Cambridge, UK) at 4°C overnight, and then incubated with the specified secondary antibodies for 1 hour. Nuclei were counterstained with DAPI, and the coverslips were mounted on a glass slide. Images were captured with a LSM 5 EXCITER confocal imaging system (Carl Zeiss, Oberkochen, Germany).

Western Blot Analysis

Western blot analysis was performed as described previously [33]. Briefly, cells were harvested, washed with PBS, and lysed in RIPA buffer. Proteins were separated by 10% sodium dodecyl sulfate–polyacrylamide gel electrophoresis and transferred to nitrocellulose membranes. Primary antibodies against p-κBα (Abcam), IκBα (Abcam), p65 (Cell Signaling Technology, Beverly, MA), p-p65 (Cell Signaling Technology), β-catenin (Cell Signaling Technology), OCN (Abcam), and GAPDH (Abcam) were diluted 1:1,000. The intensities of the bands were quantified using ImageJ software (<http://rsb.info.nih.gov/ij/>). The background was subtracted, and the signal of each target band was normalized to that of the GAPDH band.

Cell Fractionation

For the fractionation assay, cytoplasmic and nuclear RNAs were performed using a Nuclei Isolation Kit (KeyGEN, Nanjing, China). Briefly, cells were harvested and resuspended in lysis

buffer. Then, the lysate was treated with Reagent A, incubated on ice for 15 minutes, followed by centrifugation at 4°C. The pellet was then resuspended in lysis buffer followed by centrifugation. The supernatant was transferred to a new tube as the cytoplasmic fraction; the pellet was resuspended in Medium Buffer A and then added to a new tube with Medium Buffer B, followed by centrifugation at 4°C. The supernatant was saved as the cytoplasmic fraction. The pellet was used as the nuclear fraction. RNA was extracted from both fractions using Trizol.

Chromatin Immunoprecipitation

Chromatin immunoprecipitation (ChIP) assay was performed using an EZ-Magna ChIP assay kit (Merck Millipore, Darmstadt, Germany) according to manufacturer's instructions. Briefly, cells were cross-linked with 1% formaldehyde, collected, lysed, and sonicated to shear DNA. Then the DNA-protein complexes were isolated with antibodies against p65 (Abcam), or isotype IgG (Santa Cruz Biotechnology, Santa Cruz, CA). The protein/DNA complexes were then eluted and reverse cross-linked. Spin columns were used to purify the DNA. The precipitated DNA was quantified by polymerase chain reaction. Relative enrichment is calculated as the amount of amplified DNA normalized to input and relative to values obtained after normal IgG immunoprecipitation. The primers used are listed in Supporting Information Table 1.

RNA Immunoprecipitation

RNA immunoprecipitation (RIP) was performed with RNA-Binding Protein Immunoprecipitation Kit (Merck Millipore) according to the manufacturer's instructions. Briefly, magnetic beads were incubated with antibodies against p65 (Abcam), p50 (Abcam), IκBα (Abcam), and IgG control (from the kit). A 50 μl sample from the 500 μl beads suspension for each antibody was used to test the efficiency of immunoprecipitation by Western blot. The cells were collected for lysis in RIP Lysis buffer. The lysate was immunoprecipitated with different bead-antibody complexes. RNA was recovered with TRIzol and analyzed by qRT-PCR. The results were normalized relative to the input control.

RNA pull-down Assay

RNA pull-down and deletion mapping were performed as previously described [35, 36]. A series of deletion mutants of the *MIR31HG* were constructed by bioBAY Co. (Suzhou, China). Briefly, biotinylated RNAs were prepared with T4 RNA polymerase (Roche, Basel, Switzerland) and Biotin RNA labeling Mix (Roche). The labeled RNA was captured with streptavidin magnetic beads. Cell lysates or human recombinant p65 protein (Sino Biological, Beijing, China), IκBα protein (Sino Biological), and p50 protein (Enzo Life Sciences, Farmingdale, NY) were prepared and incubated with the labeled RNA at 4°C. Then, RNA-binding protein complexes were washed and eluted. A magnetic stand was used to collect the beads and the supernatant was collected for Western blot analysis.

Fluorescent In Situ Hybridization

In situ hybridization was performed with a Fluorescent In Situ Hybridization (FISH) Kit (RiboBio, Guangzhou, China). Cells were briefly rinsed in PBS and fixed in 4% formaldehyde for 10 minutes. Then the cells were permeabilized in PBS containing 0.5% Triton X-

100 at 4°C for 5 minutes, washed with PBS three times for 5 minutes, and prehybridized at 37°C for 30 minutes before hybridization. Then an anti-*MIR31HG*, anti-U6, or anti-18S oligodeoxynucleotide probe was used in the hybridization solution at 37°C overnight in the dark. The next day, the cells were counterstained with DAPI and imaged using a confocal laser-scanning microscope (Carl Zeiss).

Colocalization of lncRNA and Protein

Colocalization analysis of *MIR31HG* and $\text{I}\kappa\text{B}\alpha$ was performed as described previously [24]. The cells were hybridized with an anti-*MIR31HG* probe (RiboBio). Then the cells were rinsed briefly in PBS and incubated with an $\text{I}\kappa\text{B}\alpha$ antibody (Abcam) at 4°C overnight. The next day, the cells were incubated in the specified secondary antibodies and counterstained with DAPI. Images were obtained with a confocal laser-scanning microscope (Carl Zeiss).

Microarray and Bioinformatics

Total RNA was isolated from hASCs transfected with sh*MIR31HG* and shNC. Biotinylated cDNA was prepared according to the standard Affymetrix protocol from 250 ng total RNA by using the Ambion WT Expression Kit (Life Technologies). Following labeling, 5.5 μg of cDNA was hybridized for 16 hour at 45°C on a GeneChip Human Transcriptome Array 2.0. GeneChips were washed and stained in the Affymetrix Fluidics Station 450. GeneChips were scanned by using the Affymetrix GeneChip Command Console installed in the GeneChip Scanner 3000 7G. Data were analyzed with robust multichip analysis (RMA) algorithm using Affymetrix default analysis settings. Values presented are log₂ RMA signal intensity. For calling of differentially expressed genes, the fold differences (≥ 1.5), FDR (< 0.001) and average expression were used. For the Gene Ontology enrichment and KEGG pathway analysis, the DAVID webserver (<http://david.ncifcrf.gov/>) was used.

In Vivo Heterotopic Bone Formation Assay

The hASCs were induced under OM for 1 week before the in vivo study. The cells were resuspended and incubated with 7 mm \times 5 mm \times 2 mm Bio-Oss Collagen (Geistlich, GEWO GmbH, Baden-Baden, Germany) scaffolds for 1 hour at 37°C followed by centrifugation at 150g for 5 minutes, and then implanted subcutaneously on the back of 5-week-old BALB/c homozygous nude (nu/nu) mice (five mice per group), as described previously [28, 29, 37, 38]. Implants were harvested after 8 weeks and fixed in 4% paraformaldehyde. All animal experiments were approved by the Peking University Animal Care and Use Committee.

Hematoxylin and Eosin Staining, Masson's Trichrome, and Immunohistochemical Analysis

The specimens were decalcified in 10% ethylene diamine tetraacetic acid (pH 7.4) for 1 month, followed by dehydration and embedding in paraffin. Sections (5 μm) were cut and stained with hematoxylin and eosin (H&E) and Masson's trichrome. Meanwhile, sections were evaluated by immunohistochemical analysis, as described previously [34]. The specimens were blocked with 5% normal goat serum for 30 minutes and

then incubated with primary antibody against OCN (Santa Cruz Biotechnology) at 4°C overnight. Then, sections were processed using the ABC detection kit (Vector Laboratories, Burlingame, CA) and visualized under an Olympus microscope (Olympus Co., Tokyo, Japan).

Statistical Analysis

Statistical analyses were performed using SPSS 16.0 (SPSS, Chicago, IL). All data are expressed as the mean \pm standard deviation (SD). Differences between groups were analyzed using Student's *t* test. In cases of multiple-group testing, one-way analysis of variance was conducted. A two-tailed value of $p < .05$ was considered statistically significant.

RESULTS

TNF- α and IL-17 Inhibit Osteoblast Differentiation by Activating NF- κB

To confirm the effect of inflammatory cytokines on the OB differentiation of hASCs, we treated the cells with exogenous TNF- α (10 ng/ml) or IL-17 (10 ng/ml) under osteogenic induction. TNF- α and IL-17 significantly inhibited ALP expression and activity (Fig. 1A). The mRNA expression of osteogenic markers, runt-related transcription factor 2 (*RUNX2*) and osterix (*OSX*), was also significantly reduced by TNF- α and IL-17 (Fig. 1B). When cells were treated with TNF- α and IL-17, the ALP expression and activity and the osteogenic gene expression were further suppressed (Fig. 1A, 1B).

Further, we detected the NF- κB signaling by Western blot analysis. NF- κB dimers (predominantly p65/p50 dimers) are present in the cytoplasm in a transcriptionally inactive form due to their interactions with the $\text{I}\kappa\text{B}$ [39]. TNF- α and IL-17 rapidly activated the phosphorylation of $\text{I}\kappa\text{B}\alpha$ in 5 minutes, and its level returned to normal after 60 minutes, while total $\text{I}\kappa\text{B}\alpha$ was rapidly reduced in 5 minutes, and returned to normal level after 30 minutes (Fig. 1C). Once dissociated from $\text{I}\kappa\text{B}$, p65 undergoes phosphorylation, enters the nucleus, and initiates transcription [40]. Activated NF- κB signaling pathway has been found to promote the degradation of β -catenin [15], which is a component of the Wnt signaling and plays essential roles in bone formation. Consistently, after TNF- α and IL-17 treatment, we found that p65 was rapidly phosphorylated (Fig. 1C) and the total β -catenin expression was gradually reduced (Fig. 1D).

To further confirm the inflammatory cytokines inhibit osteogenic differentiation of hASCs via NF- κB and β -catenin pathway, we used BAY117082 (BAY) to block the activation of NF- κB , and Lithium chloride (LiCl) to block the degradation of β -catenin. The inhibition of osteogenesis induced by TNF- α and IL-17 was reverted when BAY or LiCl was used (Fig. S1A and S1B).

lncRNA *MIR31HG* Is Upregulated by Inflammatory Cytokines via NF- κB Signaling

To investigate whether lncRNA *MIR31HG* is affected under inflammatory environment, we assessed its expression in hASCs treated with TNF- α or IL-17. The qRT-PCR results showed that *MIR31HG* was significantly upregulated and displayed an oscillation pattern consistent with TNF- α and IL-17 stimulation patterns (Fig. 2A).

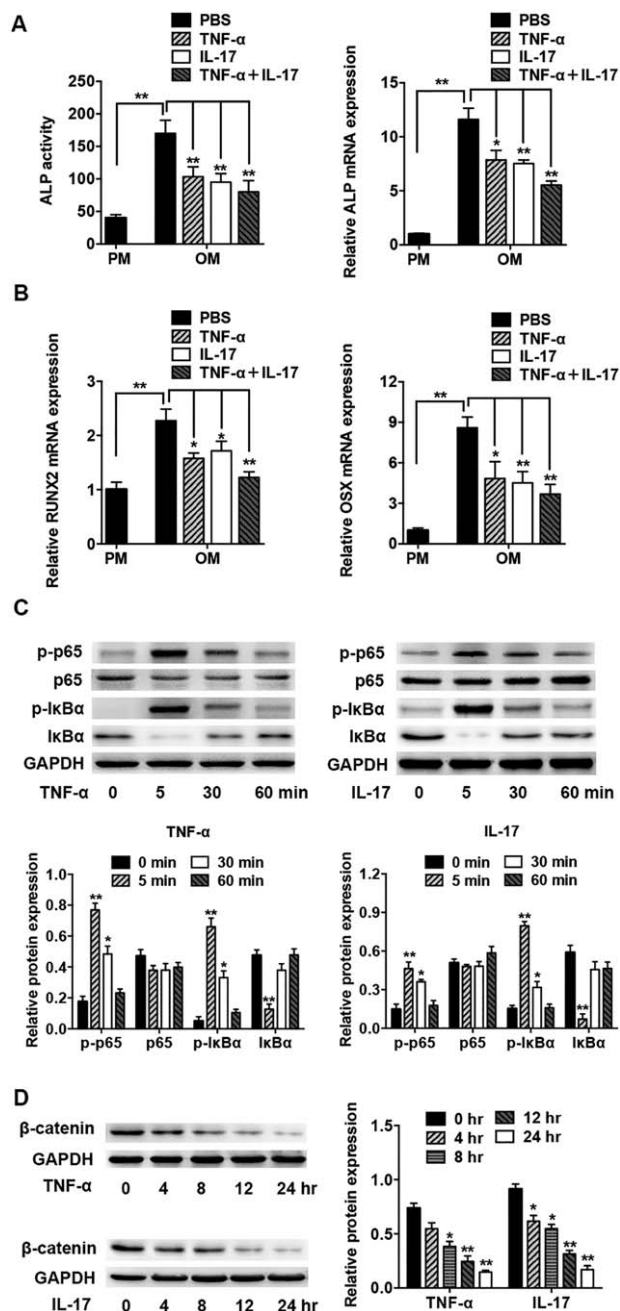


Figure 1. TNF- α and IL-17 inhibit osteoblast (OB) differentiation by activating NF- κ B signaling. hASCs were treated with exogenous TNF- α (10 ng/ml) and/or IL-17 (10 ng/ml). (A) ALP activity and mRNA expression on day 7 of OB induction. (B) Relative mRNA expression of *RUNX2* and *OSX* measured by qRT-PCR on day 7 of OB induction. GAPDH was used for normalization. (C) Western blot of protein expression of p-p65, p65, p-I κ B α , I κ B α , and the internal control GAPDH in hASCs treated with TNF- α or IL-17 for 0, 5, 30, and 60 min. Histograms show the quantification of band intensities. (D) Western blot of protein expression of β -catenin and the internal control GAPDH in hASCs treated with TNF- α or IL-17 for 0, 4, 8, 12, and 24 h. Histograms show the quantification of band intensities. Results are presented as the mean \pm SD (* p < .05, ** p < .01). Abbreviations: hASC, human adipose-derived stem cell; TNF- α , tumor necrosis factor- α ; IL-17, interleukin-17; ALP, alkaline phosphatase; *RUNX2*, runt-related transcription factor 2; *OSX*, osterix; qRT-PCR, quantitative reverse transcription-polymerase chain reaction; GAPDH, glyceraldehyde-3-phosphate dehydrogenase.

As proinflammatory cytokines drive NF- κ B activation, allowing its nuclear translocation and DNA binding to regulate gene expression, we sought to investigate whether NF- κ B signaling is directly responsible for the induced *MIR31HG* transcription. The upstream elements of the *MIR31HG* promoter were analyzed using the web-based transcription factor search site (<http://jaspar.binf.ku.dk/>) in the region between -2,000 bp upstream and +204 bp downstream from the start site of *MIR31HG*. Five putative typical p65-binding sites were identified (Fig. S2). ChIP assays were performed with an antibody against the p65 subunit of NF- κ B and six pairs of primers flanking the region of the predicted p65 binding sites (Fig. 2B). Under basal conditions, minimal p65 was bound to the promoter of *MIR31HG*. However, following TNF- α and IL-17 treatment, p65 preferentially bound to the promoter elements in the region containing the primers Ch-1, Ch-2, and Ch-3 (Fig. 2B), indicating that the distal -1,000 bp region contains an NF- κ B response element.

To determine the p65 binding sites in *MIR31HG* promoter, the full-length or truncated promoter regions were then cloned upstream of the firefly luciferase coding region (Fig. 2C). TNF- α and IL-17 treatment significantly increased the full-length *MIR31HG* promoter (P1) activity and removal of the distal -1,000 bp region (P2) lacked efficient promoter activity. Luciferase activity was increased only when the -1,957/-925 bp region (P3 and P4) was present, while deletion of this region (P5) resulted in a loss of promoter activity (Fig. 2C). This finding suggests that the -1,957/-925 bp region is the core promoter containing the NF- κ B response element.

lncRNA *MIR31HG* Inhibits Osteoblast Differentiation of hASCs

Since *MIR31HG* is induced by inflammatory cytokines, we then investigated its role in regulating the differentiation of hASCs. The qRT-PCR results showed that *MIR31HG* expression was dramatically downregulated after induction to the osteogenic lineage, and remained at a low level during osteogenesis (Fig. 3A). The mRNA expression of osteogenic markers *ALP*, *RUNX2*, and *OCN* was significantly upregulated during OB differentiation (Fig. 3A).

We then used lentivirus to overexpress or knockdown *MIR31HG* in hASCs. To control for potential off-target shRNA effects, two different sequences of shRNA directed against *MIR31HG* were used. The efficiency of lentiviral transduction was more than 80% (Fig. S3). The qRT-PCR analysis confirmed a greater than 20-fold increase in expression in the *MIR31HG* overexpression group, and a ~60% decrease in expression in the *MIR31HG* knockdown group compared with the control group (Fig. S4).

Overexpression of *MIR31HG* delayed the OB differentiation as revealed by ALP staining, ALP activity, and the mineralization assay of Alizarin red and von Kossa staining (Fig. S5A), whereas knockdown of *MIR31HG* significantly promoted the osteogenesis of hASCs (Fig. 3B). Consistently, *MIR31HG* overexpression downregulated several osteogenic markers (*ALP*, *RUNX2*, *OCN*, and *OSX*) at the mRNA level as examined by qRT-PCR (Fig. S5B), whereas knockdown of *MIR31HG* significantly upregulated the expression of these markers (Fig. 3C). Western blot and immunofluorescence staining indicated that the protein level of *OCN* was reduced in *MIR31HG* overexpressed cells (Fig. S5C and S5D) and increased in *MIR31HG* knockdown cells (Fig. 3D, 3E). Even when the cells were cultured in proliferation medium without

osteogenic supplements, knockdown of *MIR31HG* demonstrated a similar, but weaker, pro-osteogenic effect (Fig. 3B, 3C).

NF- κ B Signaling Is Inhibited by *MIR31HG* Knockdown

To understand the molecular mechanisms by which lncRNA *MIR31HG* regulates OB differentiation, we established *MIR31HG* knockdown hASCs and conducted a transcriptome microarray

analysis. Knockdown of *MIR31HG* resulted in the upregulation of 364 genes and the downregulation of 495 genes (Fig. 4A). Interestingly, *MIR31HG* knockdown led to the downregulation of genes within important signaling pathways, including the NF- κ B signaling pathway (Fig. 4B; Fig. S6). The expression of NF- κ B targets, such as IL-6, IL-7, IL-11, and TNF- α were significantly reduced (Fig. 4C; Fig. S6), as confirmed by qRT-PCR (Fig. 4D). Moreover, we found that the NF- κ B activity induced by TNF- α and IL-17 was reduced by ~60% in cells with *MIR31HG* knockdown (Fig. 4E). Consistently, confocal microscopy showed that p65 nuclear translocation induced by TNF- α and IL-17 stimulation was suppressed in *MIR31HG* knockdown cells (Fig. 4F). Finally, downstream β -catenin degradation induced by TNF- α and IL-17 was eliminated in *MIR31HG* knockdown hASCs (Fig. 4G).

lncRNA *MIR31HG* Directly Binds to I κ B α and Participates in Its Phosphorylation and NF- κ B Activation

To further study the underlying mechanism by which *MIR31HG* regulates NF- κ B signaling, we analyzed the distribution of *MIR31HG* by confocal microscopy using FISH under physiological and inflammatory conditions. In control cells (physiological conditions), *MIR31HG* was found to be located in both the nucleus and the cytoplasm (Fig. 5A). However, following TNF- α and IL-17 stimulation, *MIR31HG* was almost exclusively cytoplasmic (Fig. 5A), which was also confirmed by nuclear/cytoplasm fractionation (Fig. 5B).

The increased cytoplasmic localization of *MIR31HG* by TNF- α and IL-17 implies that the lncRNA may function in the cytoplasm. Therefore, we determined the effect of *MIR31HG* on the activation of NF- κ B complex in cytoplasm. Western blot analysis showed that I κ B α and p65 phosphorylation induced by TNF- α and IL-17 stimulation was eliminated in *MIR31HG* knockdown hASCs (Fig. 5C).

The function of most lncRNAs depends on their ability to interact with proteins [21, 22]. As *MIR31HG* may function by interacting with the NF- κ B:I κ B complex, we performed an RIP assay using antibodies against p65, p50, or I κ B α . All three antibodies retrieved significant amounts of *MIR31HG* RNA and NF- κ B:I κ B complex. However, successful knockdown of I κ B α (Fig. S7) eliminated *MIR31HG* enrichment in p65 or p50 immunoprecipitates, but

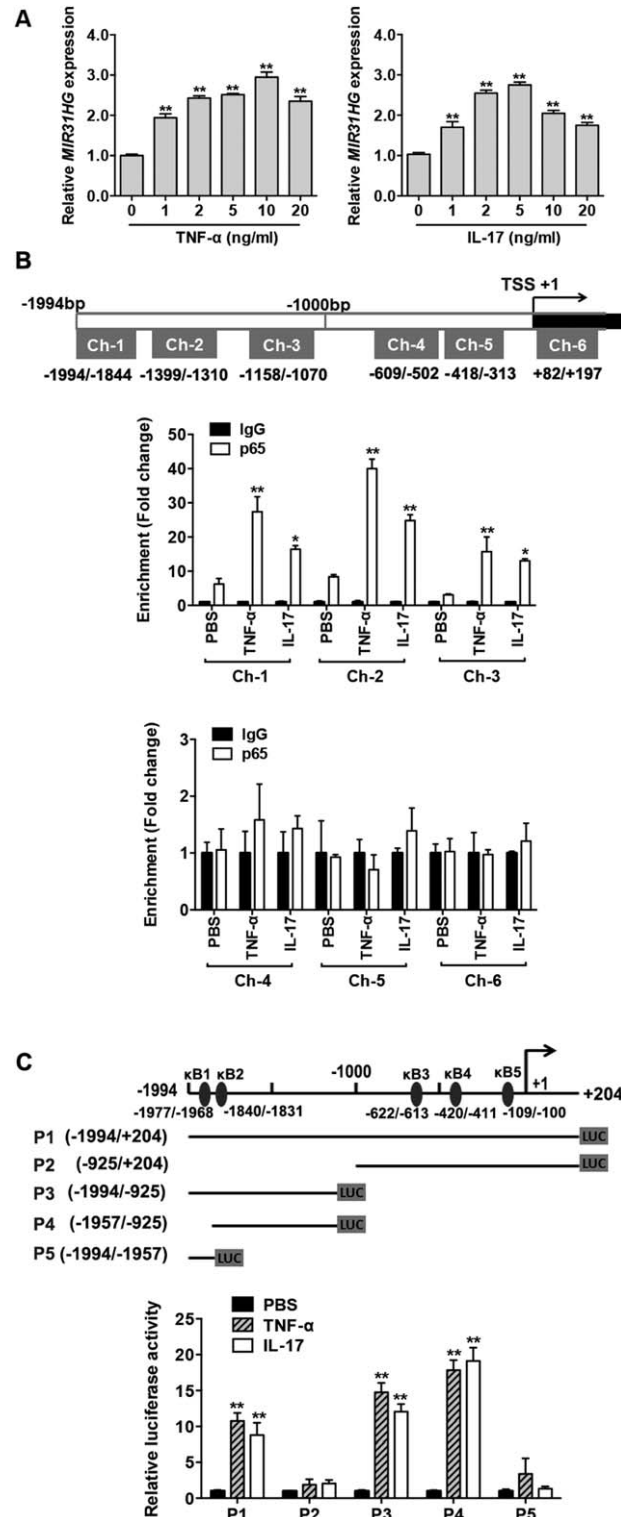


Figure 2. NF- κ B induces *MIR31HG* expression. (A) Relative expression of *MIR31HG* in hASCs stimulated with TNF- α or IL-17 for the concentration indicated (by qRT-PCR; normalized by GAPDH; relative to untreated groups). (B) Upper: Diagram of the *MIR31HG* promoter and location of the primers. Positions marked are relative to the transcriptional start site (TSS). Lower: ChIP-qPCR showing the interaction between the p65 subunit and the *MIR31HG* promoter in hASCs untreated or treated with TNF- α or IL-17 for 4 h. IgG was used for normalization. (C) Upper: Schematic maps representing the five potential binding sites of p65 in the *MIR31HG* promoter and the four deletion mutants of the *MIR31HG* promoter. The arrow indicates the position of the TSS +1. Lower: Luciferase activity of 293T cells transfected with luciferase constructs containing full-length (P1) or truncated forms (P2–P5) of the *MIR31HG* promoter. The ratio of firefly luciferase to renilla luciferase activity was calculated and normalized to that of cells treated with PBS. Results are presented as the mean \pm SD (* p < .05, ** p < .01). Abbreviations: TNF- α , tumor necrosis factor- α ; IL-17, interleukin-17; qRT-PCR, quantitative reverse transcription-polymerase chain reaction; GAPDH, glyceraldehyde-3-phosphate dehydrogenase; ChIP, Chromatin immunoprecipitation; hASC, human adipose-derived stem cell.

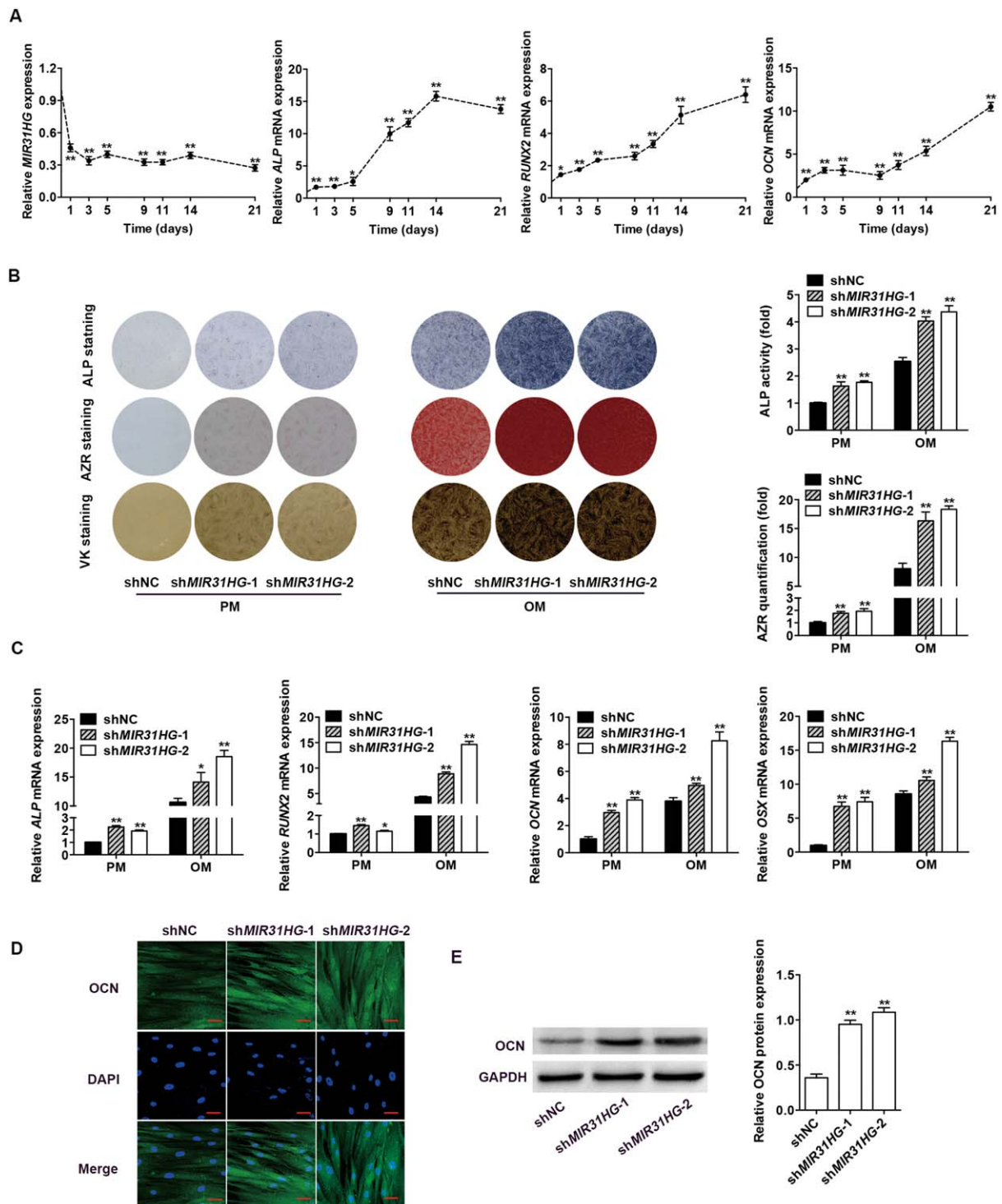


Figure 3. *MIR31HG* knockdown promotes osteoblast (OB) differentiation of hASCs. (A) Relative expression of *MIR31HG*, *ALP*, *RUNX2*, and *OCN* during OB differentiation of hASCs (by qRT-PCR; normalized by GAPDH; relative to day 0 groups). (B) Images of ALP, Alizarin red (AZR), and von Kossa (VK) staining in shNC, shMIR31HG-1, and shMIR31HG-2 groups. Cells were cultured in proliferation medium (PM) or osteogenic medium (OM). Histograms show ALP activity and quantification of AZR staining by spectrophotometry. (C) Relative mRNA expression of *ALP*, *RUNX2*, *OCN*, and *OSX* measured by qRT-PCR on day 14 of OB induction. GAPDH was used for normalization. (D) Confocal microscopy of OCN with DAPI counterstaining in shNC, shMIR31HG-1, and shMIR31HG-2 groups after induction to the osteogenic lineage on day 14. Scale bars: 50 μ m. (E) Western blot of protein expression of OCN and the internal control GAPDH on day 14 of OB induction. Histograms show the quantification of band intensities. Results are presented as the mean \pm SD (* p < .05, ** p < .01). Abbreviations: hASC, human adipose-derived stem cell; ALP, alkaline phosphatase; *RUNX2*, runt-related transcription factor 2; OCN, osteocalcin; qRT-PCR, quantitative reverse transcription-polymerase chain reaction; GAPDH, glyceraldehyde-3-phosphate dehydrogenase; shNC, scramble control; *OSX*, osterix.

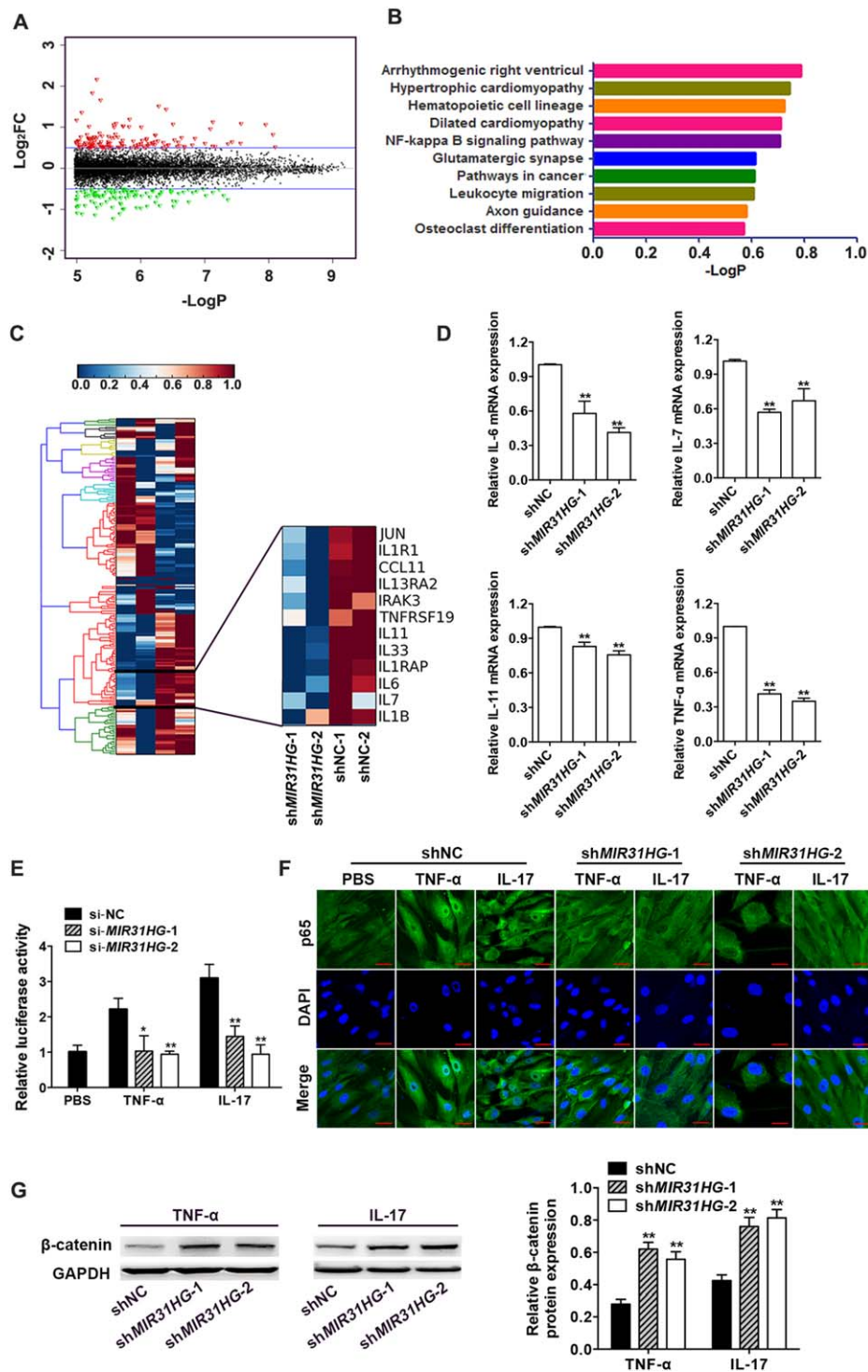


Figure 4. NF- κ B signaling is inhibited by *MIR31HG* knockdown. **(A)** Volcano plot showed that a total of 364 genes were upregulated and 495 genes were downregulated in *MIR31HG* knockdown hASCs. **(B)** Kyoto Encyclopedia of Genes and Genomes analysis showed that the differentially expressed genes were enriched in the NF- κ B signaling pathway. **(C)** Heat map from microarray data showing the differentially expressed genes within the NF- κ B signaling pathway. **(D)** Relative mRNA expression of IL-6, IL-7, IL-11, and TNF- α measured by qRT-PCR. GAPDH was used for normalization. **(E)** The 293T cells were co-transfected with scramble siRNA (si-NC) or *MIR31HG* siRNA (si-*MIR31HG*-1 and si-*MIR31HG*-2) and NF- κ B luciferase reporter, and stimulated with TNF- α or IL-17 for 24 h. Luciferase activity was measured and normalized by renilla luciferase activity. **(F)** Immunofluorescent confocal microscopy of p65 nuclear translocation in hASCs expressing shNC, sh*MIR31HG*-1, or sh*MIR31HG*-2, treated with TNF- α or IL-17 for 24 h. Scale bars: 20 μ m **(G)** Western blot of protein expression of β -catenin and the internal control GAPDH in hASCs expressing shNC, sh*MIR31HG*-1, or sh*MIR31HG*-2 treated with TNF- α or IL-17 for 24 h. Histograms show the quantification of band intensities. Results are presented as the mean \pm SD ($*p < .05$, $**p < .01$). Abbreviations: hASC, human adipose-derived stem cell; IL-6, interleukin-6; IL-7, interleukin-7; IL-11, interleukin-11; qRT-PCR, quantitative reverse transcription-polymerase chain reaction; TNF- α , tumor necrosis factor- α ; IL-17, interleukin-17; shNC, scramble control; GAPDH, glyceraldehyde-3-phosphate dehydrogenase

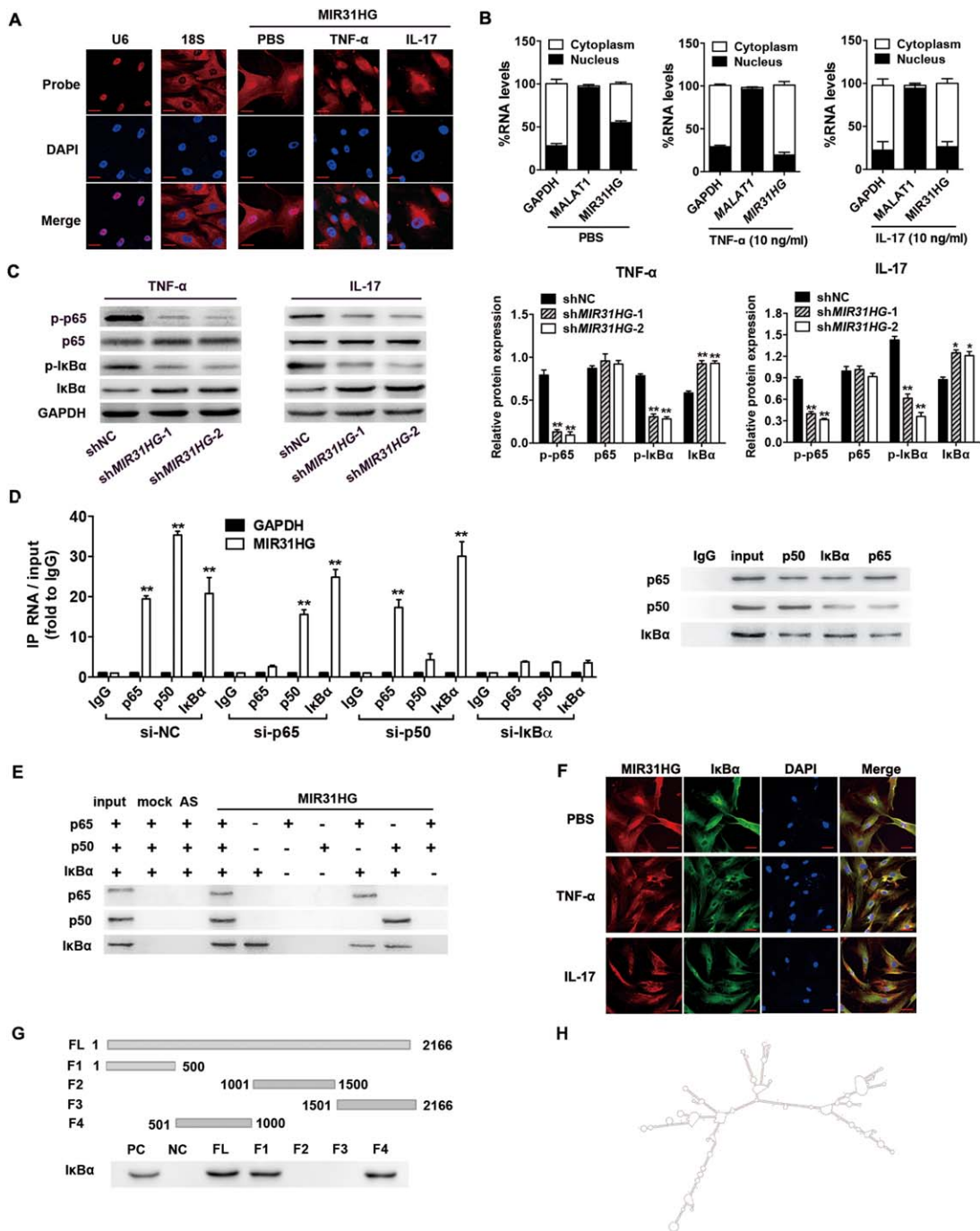


Figure 5. *MIR31HG* directly binds to IκBα and participates in IκBα phosphorylation. (A) Confocal FISH images showing localization of *MIR31HG* in hASCs unstimulated or stimulated with TNF-α and IL-17 for 24 h. 18S, probe for 18S rRNA; U6, probe for U6 snRNA. Scale bars: 20 μm (B) Percentage of nuclear and cytoplasmic RNA levels of *MIR31HG*, *MALAT1*, and *GAPDH* measured by qRT-PCR after subcellular fractionation in hASCs untreated or treated with TNF-α and IL-17 for 24 h. (C) Western blot of protein expression of p-p65, p65, p-IκBα, IκBα, and the internal control *GAPDH* in hASCs expressing shNC, sh*MIR31HG*-1, or sh*MIR31HG*-2 treated with TNF-α or IL-17 for 30 min. Histograms show the quantification of band intensities. (D) Left: RIP using p65, p50, or IκBα antibody followed by qRT-PCR for *MIR31HG* in hASCs transfected with scramble siRNA (si-NC), p65 siRNA (si-p65), p50 siRNA (si-p50), or IκBα siRNA (si-IκBα). Right: Western blot showing p65, p50, or IκBα antibody retrieved p65:p50:IκBα complex in hASCs. (E) RNA pull-down showing *MIR31HG* binding capacity to IκBα in hASCs. AS, antisense. (F) Confocal FISH images of colocalization of *MIR31HG* and IκBα in hASCs with or without TNF-α or IL-17 treatment. Scale bars: 50 μm. (G) Upper: Schematic maps representing four deleted *MIR31HG* mutants (F1–F4). Lower: RNA pull-down showing deleted *MIR31HG* mutants binding capacity to IκBα. PC, positive control; NC, negative control; FL, full-length. (H) Prediction of *MIR31HG* structure of 1–1,000 nt region by RNA folding analyzes software (Mfold, <http://unafold.rna.albany.edu/?q=mfold>). Results are presented as the mean ± SD (**p* < .05, ***p* < .01). Abbreviations: FISH, Fluorescent In Situ Hybridization; hASC, human adipose-derived stem cell; TNF-α, tumor necrosis factor-α; IL-17, interleukin-17; *GAPDH*, glyceraldehyde-3-phosphate dehydrogenase; qRT-PCR, quantitative reverse transcription-polymerase chain reaction.

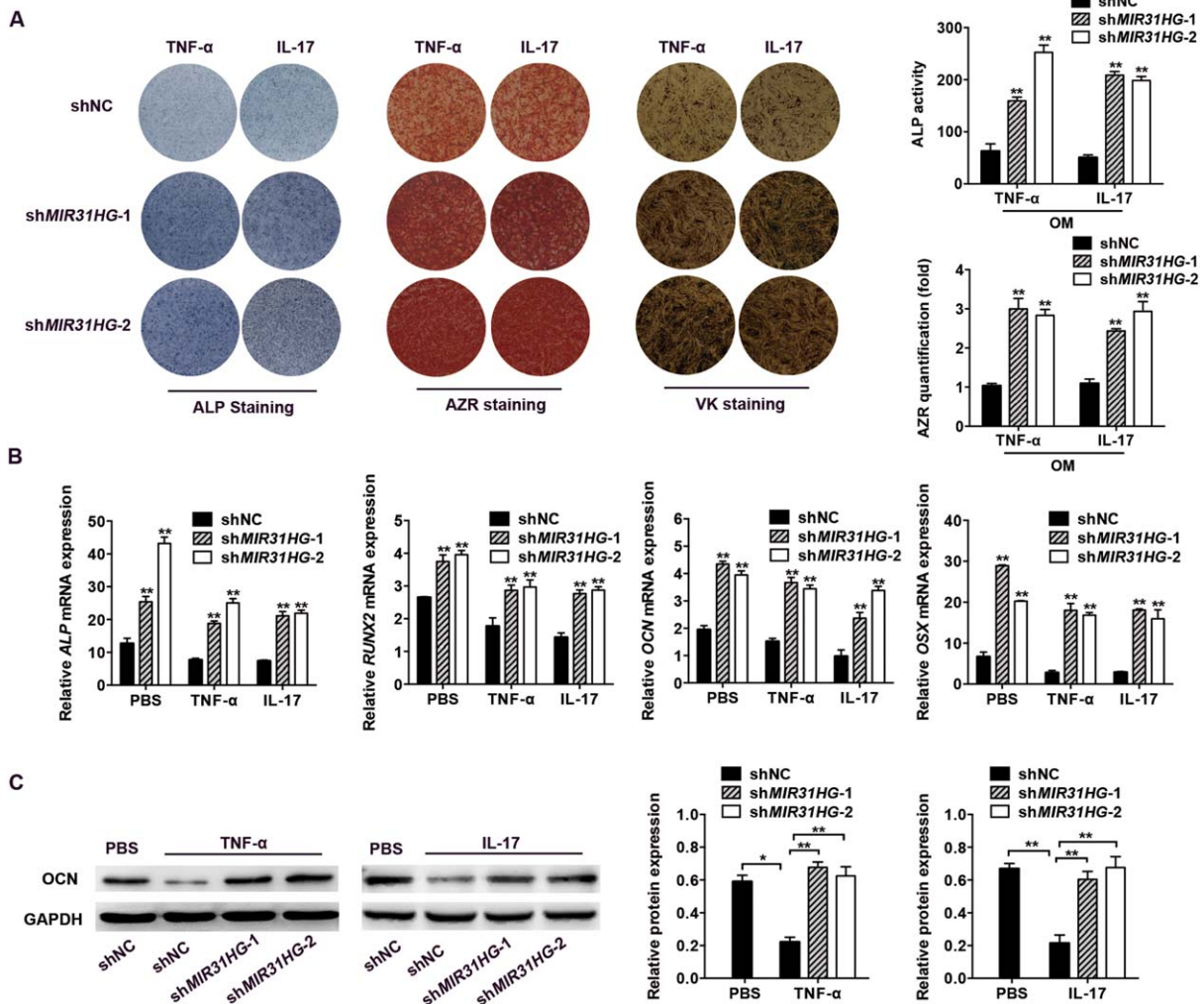


Figure 6. *MIR31HG* knockdown reverses the inhibition of osteogenic differentiation induced by TNF- α and IL-17. Cells were treated with TNF- α (10 ng/ml) or IL-17 (10 ng/ml) during osteogenic differentiation. (A) Images of ALP, Alizarin red (AZR), and von Kossa (VK) staining in shNC, sh*MIR31HG*-1, and sh*MIR31HG*-2 groups treated with TNF- α or IL-17. Histograms show ALP activity and quantification of AZR staining by spectrophotometry. (B) Relative mRNA expression of *ALP*, *RUNX2*, *OCN*, and *OSX* measured by qRT-PCR in shNC, sh*MIR31HG*-1, and sh*MIR31HG*-2 groups with or without TNF- α or IL-17 treatment on day 14 of OB induction. GAPDH was used for normalization. (C) Western blot of protein expression of *OCN* and the internal control *GAPDH* in shNC, sh*MIR31HG*-1, and sh*MIR31HG*-2 groups with or without TNF- α or IL-17 treatment on day 14 of OB induction. Histograms show the quantification of band intensities. Results are presented as the mean \pm SD (* p < .05, ** p < .01). Abbreviations: TNF- α , tumor necrosis factor- α ; IL-17, interleukin-17; shNC, scramble control; ALP, alkaline phosphatase; *RUNX2*, runt-related transcription factor 2; *OCN*, osteocalcin; *OSX*, osterix; qRT-PCR, quantitative reverse transcription-polymerase chain reaction; *GAPDH*, glyceraldehyde-3-phosphate dehydrogenase.

successful knockdown of p65 or p50 (Fig. S7) did not affect *MIR31HG* enrichment in $\text{I}\kappa\text{B}\alpha$ immunoprecipitates (Fig. 5D). We further performed an RNA pull-down assay using in vitro-generated biotinylated full-length *MIR31HG* transcripts. Consistently, *MIR31HG* transcripts pulled down substantial amounts of p65, p50, and $\text{I}\kappa\text{B}\alpha$ (Fig. 5E). However, *MIR31HG* transcripts cannot retrieve p65 and p50 in $\text{I}\kappa\text{B}\alpha$ knockdown cells (Fig. S8). Furthermore, confocal microscopy for *MIR31HG* FISH and $\text{I}\kappa\text{B}\alpha$ immunostaining showed colocalization of *MIR31HG* and $\text{I}\kappa\text{B}\alpha$ in the cytoplasm (Fig. 5F).

To further map the binding domain, a series of deletion mutants of *MIR31HG* were generated. According to the RNA folding analyzes software (Mfold, <http://unafold.rna.albany.edu/?q=mfold>) [41], *MIR31HG* contains several functional domains (Fig. S9). We generated four *MIR31HG* deletion

mutants and tested their binding capacity with $\text{I}\kappa\text{B}\alpha$. Interestingly, mutants containing 1–500 nt and 501–1,000 nt (F1 and F2) were sufficient to bind $\text{I}\kappa\text{B}\alpha$, while other deletion mutants without this fragment (F3 and F4) lost the binding capacity (Fig. 5G). The Mfold software [41] indicated stable stem-loop structures within 1–1,000 nt (Fig. 5H), which might provide the necessary spatial conformation for the interaction.

Knockdown of *MIR31HG* Reverses the Inhibition of OB Differentiation Induced by TNF- α and IL-17

Since lncRNA *MIR31HG* builds a regulation circuitry with NF- κB , we investigated the effect of *MIR31HG* knockdown on osteogenesis under stimulated inflammatory conditions. The inhibition of OB differentiation induced by TNF- α and IL-17 was reversed by knockdown of *MIR31HG*, as shown by ALP

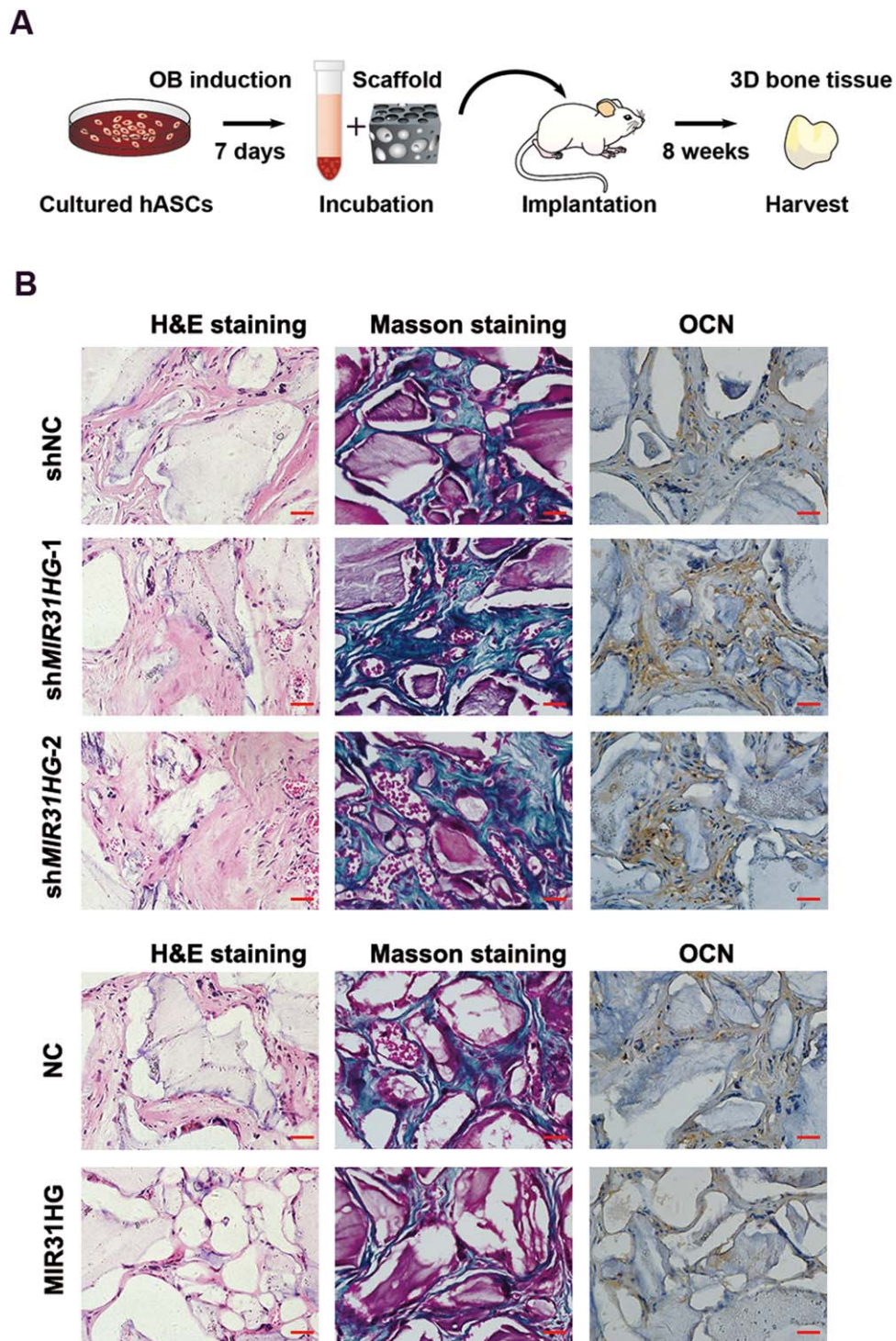


Figure 7. *MIR31HG* knockdown promoted heterotopic bone formation in vivo. (A) Schematic diagram illustrating the experimental set-up. (B) H&E staining, Masson's trichrome staining, and immunohistochemical staining of OCN in shNC, shMIR31HG-1, shMIR31HG-2, NC, and *MIR31HG* groups. Scale bar: 50 μ m. Abbreviations: OCN, osteocalcin; shNC, scramble control.

staining, ALP activity, and mineralized matrix staining (Fig. 6A). The downregulated mRNA expression of *ALP*, *RUNX2*, *OCN*, and *OSX* by TNF- α and IL-17 treatment was rescued by *MIR31HG* knockdown (Fig. 6B). The inhibition of OCN protein expression induced by TNF- α and IL-17 treatment was reversed in *MIR31HG* knockdown cells (Fig. 6C).

Knockdown of *MIR31HG* Promotes Bone Formation In Vivo

To clarify whether downregulation of *MIR31HG* can enhance bone formation in vivo, hASCs expressing shMIR31HG, *MIR31HG* and the control were loaded on Bio-Oss Collagen scaffolds, and implanted in the subcutaneous tissue of nude

mice (five mice per group). The study plan is given in Figure 7A. After 8 weeks, the implantation samples were harvested and analyzed. The amount of bone tissue in H&E staining and collagen organization with blue color in Masson's trichrome staining was significantly higher in implants containing *MIR31HG* knockdown cells and thinner in the *MIR31HG* group. Meanwhile, the osteoblasts and bone trabeculae were positive for OCN, as observed in immunohistochemical staining. The size and intensity of staining were increased in the *MIR31HG* knockdown group and decreased in the *MIR31HG* group (Fig. 7B).

DISCUSSION

In this study, we demonstrated that knockdown of *MIR31HG* not only enhanced the osteogenic differentiation, but also sufficiently reversed the inhibition of osteogenesis in inflammatory environment. Numerous genes and several signaling pathways are involved in the lineage commitment of hASCs to osteoblasts, and some lncRNAs have been shown to regulate osteogenesis of MSCs [42–45], but none of these lncRNAs are demonstrated in inflammatory environment. In therapeutic bone regeneration, the defective or injured tissues are frequently associated with abnormal inflammatory and protein mediators [5]. Bone formation is compromised under pathogenic conditions of chronic inflammation [13]. Thus, knockdown of *MIR31HG* may serve as a promising approach to improve osteogenesis under an inflamed microenvironment in bone repair and regeneration.

Mechanistically, we found that the cytoplasmic lncRNA *MIR31HG* directly bound to $\text{I}\kappa\text{B}\alpha$ and participated in its phosphorylation and NF- κB activation. *MIR31HG* was physically associated with $\text{I}\kappa\text{B}\alpha$ as determined by RIP and RNA pull-down assay, and silencing $\text{I}\kappa\text{B}\alpha$ eliminated the affinity of *MIR31HG* for the NF- κB : $\text{I}\kappa\text{B}$ complex. The phosphorylation of $\text{I}\kappa\text{B}\alpha$ and activation of NF- κB pathway relied on the function of lncRNA *MIR31HG*. The complex secondary and higher-order structures of lncRNA extend their capability to interact with protein complexes [21, 22, 46, 47]. According to the RNA folding analysis, the 1–500 nt fragment and 501–1,000 nt fragment of *MIR31HG* contained stable stem-loop structures, which were the core $\text{I}\kappa\text{B}\alpha$ binding domains. Consistently, previous study have identified a lncRNA function in the similar way, lncRNA *NKILA* binds to p65 and directly inhibits IKK-induced $\text{I}\kappa\text{B}$ phosphorylation by masking the phosphorylation sites of $\text{I}\kappa\text{B}$ from IKK [24]. However, the precise molecular mechanism by which the *MIR31HG* domain acts on $\text{I}\kappa\text{B}\alpha$ phosphorylation is not fully understood, but the result of this study does imply the role of *MIR31HG* in activation of NF- κB pathway. Additionally, according to the microarray analysis, several important signaling pathways were also regulated by *MIR31HG*. Therefore, we could not exclude the possibility that *MIR31HG* interact with other signaling pathways to regulate bone formation.

Interestingly, we also found that the expression of *MIR31HG* was upregulated after NF- κB activation. There existed positive bi-directional interaction between *MIR31HG* and NF- κB . The p65 subunit bound to *MIR31HG* promoter and promoted its expression. We identified a p65 binding site located at the distal –1,000 bp upstream of *MIR31HG* transcript start site, consistent with a previous study [27]. Usually, the regulatory function of p65 depends on the manner in which it is induced and the

interacted transcription factors [48]. Although our study revealed that p65 directly bound to the *MIR31HG* promoter, previous studies have shown that the expression of *MIR31HG* can also be mediated by the activation of C/EBP- β [49], DNA methylation and chromatin acetylation [25]. Coincidentally, NF- κB p65 and C/EBP- β form a complex by direct protein/protein interaction to synergistically mediate the expression of some other genes [50], and TNF- α can increase the expression and activation of C/EBP- β [51]. Thus, other transcription factors may also be involved in upregulation of *MIR31HG* under inflamed conditions.

Even though majority of the lncRNAs remain in the nucleus and localize with their associated transcriptional regulator to DNA [52], there is evidence that some lncRNAs operate in the cytoplasm, such as *NKILA* [24] and lnc-DC [53]. Interestingly, we found that *MIR31HG* was normally diffusely distributed in nucleus, but was exported to the cytoplasm on inflammatory stimulation. Consistently, *MIR31HG* has been showed to be transported to the cytoplasm during oncogene-induced senescence [26]. Indeed, several regulatory RNAs show similar export from nucleus to cytoplasm on specific signals or stimuli, such as antisense ubiquitin carboxy terminal hydrolase L1 (AS Uchl1) lncRNA [54] and the mouse-specific CTN-RNA [55]. The transportation of RNAs on specific signals/stimuli is defined as “quick response” mechanism [56] and the transportation of *MIR31HG* may be associated with the general RNA export factor Aly [26].

In summary, we identified a lncRNA, *MIR31HG*, involved in inflammation-mediated inhibition of bone formation. Our results highlight the bi-directional interaction between lncRNA *MIR31HG* and NF- κB pathways that may attenuate osteogenic differentiation of hASCs. The growing knowledge of *MIR31HG* is pointing toward the potential use as RNA based targets for novel therapeutic approaches to inhibit inflammation and enhance bone formation in bone tissue engineering. To reach this goal, a further understanding of the functional versatility of lncRNAs in physiological conditions is required.

CONCLUSIONS

Knockdown of *MIR31HG* not only promoted osteogenic differentiation but also reversed the inflammation-induced inhibition of bone formation. *MIR31HG* is induced by nuclear translocation of NF- κB , and *MIR31HG*, in turn, directly binds to $\text{I}\kappa\text{B}\alpha$ and contributes to $\text{I}\kappa\text{B}\alpha$ phosphorylation and NF- κB activation. Inhibition of the *MIR31HG*–NF- κB regulatory circuitry may have benefits in enhancing bone regeneration and inhibiting inflammation in bone tissue engineering.

ACKNOWLEDGEMENTS

This study was financially supported by grants from the National Natural Science Foundation of China (No. 81371118, No. 81402235), the Program for New Century Excellent Talents in University from Ministry of Education of China (NCET-11-0026), the Ph.D. Programs Foundation of Ministry of Education of China (No. 20130001110101), and grants from the PKU School of Stomatology for Talented Young Investigators (PKUSS20140104).

AUTHOR CONTRIBUTIONS

C.J., L.J., Y.H.: contributed equally to this work.

DISCLOSURE OF POTENTIAL CONFLICTS OF INTEREST

The authors have no conflicts of interest to disclose.

REFERENCES

- 1 Tapp H, Hanley EN, Jr., Patt JC et al. Adipose-derived stem cells: characterization and current application in orthopaedic tissue repair. *Exp Biol Med* 2009;234:1–9.
- 2 Rada T, Reis RL Gomes ME. Adipose tissue-derived stem cells and their application in bone and cartilage tissue engineering. *Tissue Eng Part B Rev* 2009;15:113–125.
- 3 Levi B Longaker MT. Concise review: Adipose-derived stromal cells for skeletal regenerative medicine. *STEM CELLS* 2011;29:576–582.
- 4 Levi B, James AW, Nelson ER et al. Human adipose derived stromal cells heal critical size mouse calvarial defects. *PLoS One* 2010;5:e11177.
- 5 Bastian O, Pillay J, Alblas J et al. Systemic inflammation and fracture healing. *Journal of Leukocyte Biol* 2011;89:669–673.
- 6 Huebsch N, Arany PR, Mao AS et al. Harnessing traction-mediated manipulation of the cell/matrix interface to control stem-cell fate. *Nat Mater* 2010;9:518–526.
- 7 Sacchetti B, Funari A, Michienzi S et al. Self-renewing osteoprogenitors in bone marrow sinusoids can organize a hematopoietic microenvironment. *Cell* 2007;131:324–336.
- 8 Lacey DC, Simmons PJ, Graves SE et al. Proinflammatory cytokines inhibit osteogenic differentiation from stem cells: Implications for bone repair during inflammation. *Osteoarthritis Cartilage/OARS, Osteoarthritis Res Soc* 2009;17:735–742.
- 9 Huang RL, Yuan Y, Tu J et al. Opposing TNF- α /IL-1 β and BMP-2-activated MAPK signaling pathways converge on Runx2 to regulate BMP-2-induced osteoblastic differentiation. *Cell Death Dis* 2014;5:e1187.
- 10 Novack DV. Role of NF- κ B in the skeleton. *Cell Res* 2011;21:169–182.
- 11 Matzelle MM, Shaw AT, Baum R et al. Inflammation in arthritis induces expression of BMP3, an inhibitor of bone formation. *Scandinavian J Rheumatol* 2016;1–5.
- 12 Shaw AT Gravallesse EM. Mediators of inflammation and bone remodeling in rheumatic disease. *Seminars Cell Dev Biol* 2016;49:2–10.
- 13 Krum SA, Chang J, Miranda-Carboni G et al. Novel functions for NF- κ B: Inhibition of bone formation. *Nat Rev Rheumatol* 2010;6:607–611.
- 14 Chang J, Wang Z, Tang E et al. Inhibition of osteoblastic bone formation by nuclear factor- κ B. *Nat Med* 2009;15:682–689.
- 15 Chang J, Liu F, Lee M et al. NF- κ B inhibits osteogenic differentiation of mesenchymal stem cells by promoting beta-catenin degradation. *Proc Natl Acad Sci U S A* 2013;110:9469–9474.
- 16 Mattick JS. RNA regulation: A new genetics? *Nat Rev Genet* 2004;5:316–323.
- 17 Liu Y, Liu W, Hu C et al. MiR-17 modulates osteogenic differentiation through a coherent feed-forward loop in mesenchymal stem cells isolated from periodontal ligaments of patients with periodontitis. *STEM CELLS* 2011;29:1804–1816.
- 18 Yang N, Wang G, Hu C et al. Tumor necrosis factor alpha suppresses the mesenchymal stem cell osteogenesis promoter miR-21 in estrogen deficiency-induced osteoporosis. *J Bone Mineral Res* 2013;28:559–573.
- 19 Dong J, Cui X, Jiang Z et al. MicroRNA-23a modulates TNF- α -inhibited osteogenic osteoblasts apoptosis by directly targeting Fas. *J Cell Biochem* 2013;114:2738–2745.
- 20 Wu T, Xie M, Wang X et al. miR-155 modulates TNF- α -inhibited osteogenic differentiation by targeting SOCS1 expression. *Bone* 2012;51:498–505.
- 21 Hung T, Chang HY. Long noncoding RNA in genome regulation: Prospects and mechanisms. *RNA Biol* 2010;7:582–585.
- 22 Li X, Wu Z, Fu X et al. lncRNAs: Insights into their function and mechanics in underlying disorders. *Mutat Res Rev Mutat Res* 2014;762:1–21.
- 23 Rapicavoli NA, Qu K, Zhang J et al. A mammalian pseudogene lncRNA at the interface of inflammation and anti-inflammatory therapeutics. *eLife* 2013;2:e00762.
- 24 Liu B, Sun L, Liu Q et al. A cytoplasmic NF- κ B interacting long noncoding RNA blocks I κ B phosphorylation and suppresses breast cancer metastasis. *Cancer Cell* 2015;27:370–381.
- 25 Augoff K, McCue B, Plow EF et al. miR-31 and its host gene lncRNA LOC554202 are regulated by promoter hypermethylation in triple-negative breast cancer. *Mol Cancer* 2012;11:5.
- 26 Montes M, Nielsen MM, Maglieri G et al. The lncRNA MIR31HG regulates p16(INK4A) expression to modulate senescence. *Nat Commun* 2015;6:6967.
- 27 Rajbhandari R, McFarland BC, Patel A et al. Loss of tumor suppressive microRNA-31 enhances TRADD/NF- κ B signaling in glioblastoma. *Oncotarget* 2015;6:17805–17816.
- 28 Ge W, Shi L, Zhou Y et al. Inhibition of osteogenic differentiation of human adipose-derived stromal cells by retinoblastoma binding protein 2 repression of RUNX2-activated transcription. *STEM CELLS (DAYTON, OHIO)* 2011;29:1112–1125.
- 29 Ge W, Liu Y, Chen T et al. The epigenetic promotion of osteogenic differentiation of human adipose-derived stem cells by the genetic and chemical blockade of histone demethylase LSD1. *Biomaterials* 2014;35:6015–6025.
- 30 Bhargava U, Bar-Lev M, Bellows CG et al. Ultrastructural analysis of bone nodules formed in vitro by isolated fetal rat calvaria cells. *Bone* 1988;9:155–163.
- 31 Yang X, Lu H, Yan B et al. DeltaNp63 variably regulates a broad NF- κ B gene program and promotes squamous epithelial proliferation, migration, and inflammation. *Cancer Res* 2011;71:3688–3700.
- 32 Zhou H, Rigoutsos I. MiR-103a-3p targets the 5' UTR of GPRC5A in pancreatic cells. *RNA* 2014;20:1431–1439.
- 33 Jia LF, Wei SB, Gan YH et al. Expression, regulation and roles of miR-26a and MEG3 in tongue squamous cell carcinoma. *Int J Cancer* 2014;135:2282–2293.
- 34 Wei J, Li H, Wang S et al. let-7 enhances osteogenesis and bone formation while repressing adipogenesis of human stromal/mesenchymal stem cells by regulating HMGA2. *STEM CELLS Dev* 2014;23:1452–1463.
- 35 Wang L, Zhao Y, Bao X et al. lncRNA Dum interacts with Dnmts to regulate Dppa2 expression during myogenic differentiation and muscle regeneration. *Cell Res* 2015;25:335–350.
- 36 Tsai MC, Manor O, Wan Y et al. Long noncoding RNA as modular scaffold of histone modification complexes. *Science* 2010;329:689–693.
- 37 Yu BH, Zhou Q, Wang ZL. Periodontal ligament versus bone marrow mesenchymal stem cells in combination with Bio-Oss scaffolds for ectopic and in situ bone formation: a comparative study in the rat. *J Biomater Appl* 2014;29:243–253.
- 38 Lai RF, Li ZJ, Zhou ZY et al. Effect of rhBMP-2 sustained-release nanocapsules on the ectopic osteogenesis process in Sprague-Dawley rats. *Asian Pacific J Trop Med* 2013;6:884–888.
- 39 Beg AA, Ruben SM, Scheinman RI et al. I κ B interacts with the nuclear localization sequences of the subunits of NF- κ B: A mechanism for cytoplasmic retention. *Genes Dev* 1992;6:1899–1913.
- 40 Pahl HL. Activators and target genes of rel/NF- κ B transcription factors. *Oncogene* 1999;18:6853–6866.
- 41 Zuker M. Mfold web server for nucleic acid folding and hybridization prediction. *Nucl Acid Res* 2003;31:3406–3415.
- 42 Zhu L, Xu PC. Downregulated lncRNA-ANCR promotes osteoblast differentiation by targeting EZH2 and regulating Runx2 expression. *Biochem Biophys Res Commun* 2013;432:612–617.
- 43 Zhang JF, Fu WM, He ML et al. MiR-637 maintains the balance between adipocytes and osteoblasts by directly targeting Osterix. *Mol Biol Cell* 2011;22:3955–3961.
- 44 Zhuang W, Ge X, Yang S et al. Upregulation of lncRNA MEG3 promotes osteogenic differentiation of mesenchymal stem cells from multiple myeloma patients by targeting BMP4 transcription. *STEM CELLS* 2015;33:1985–1997.
- 45 Huang Y, Zheng Y, Jia L et al. Long noncoding RNA H19 promotes osteoblast differentiation via TGF- β 1/Smad3/HDAC signaling pathway by deriving miR-675. *STEM CELLS* 2015;33:3481–3492.
- 46 Batista PJ, Chang HY. Long noncoding RNAs: Cellular address codes in development and disease. *Cell* 2013;152:1298–1307.
- 47 Ulitsky I, Bartel DP. lincRNAs: Genomics, evolution, and mechanisms. *Cell* 2013;154:26–46.
- 48 Campbell KJ, Rocha S, Perkins ND. Active repression of antiapoptotic gene expression

by RelA(p65) NF-kappa B. *Mol Cell* 2004;13:853–865.

49 Xi S, Yang M, Tao Y et al. Cigarette smoke induces C/EBP-beta-mediated activation of miR-31 in normal human respiratory epithelia and lung cancer cells. *PLoS One* 2010;5:e13764.

50 Diehl AM, Yang SQ, Yin M et al. Tumor necrosis factor-alpha modulates CCAAT/enhancer binding proteins-DNA binding activities and promotes hepatocyte-specific gene expression during liver regeneration. *Hepatology* 1995;22:252–261.

51 Xia C, Cheshire JK, Patel H et al. Crosstalk between transcription factors NF-kappa B and C/EBP in the transcriptional regulation of genes. *Int J Biochem Cell Biol* 1997;29:1525–1539.

52 Sharma S, Findlay GM, Bandukwala HS et al. Dephosphorylation of the nuclear factor of activated T cells (NFAT) transcription factor is regulated by an RNA-protein scaffold complex. *Proc Natl Acad Sci U S A* 2011;108:11381–11386.

53 Wang P, Xue Y, Han Y et al. The STAT3-binding long noncoding RNA lnc-DC controls

human dendritic cell differentiation. *Science* 2014;344:310–313.

54 Carrieri C, Cimatti L, Biagioli M et al. Long non-coding antisense RNA controls Uchl1 translation through an embedded SINEB2 repeat. *Nature* 2012;491:454–457.

55 Prasanth KV, Prasanth SG, Xuan Z et al. Regulating gene expression through RNA nuclear retention. *Cell* 2005;123:249–263.

56 Singh DK, Prasanth KV. Functional insights into the role of nuclear-retained long noncoding RNAs in gene expression control in mammalian cells. *Chromosome Res* 2013;21:695–711.



See www.StemCells.com for supporting information available online.